Metallicity

Where do metals come from?

What controls the metallicity of a galaxy?

How do we measure it?

Results.

Fast terminology

"Metallicity"

For stars, usually refers to Fe

For gas, usually refers to O

Sometimes refers to all metals

X = mass fraction of Hydrogen

Y = mass fraction of Helium

Z = mass fraction of metals

"Abundance"

Usually refers to arbitrary elements

Abundance: Gas Phase

The gas phase abundance of an element X is defined:

$$\boxed{12+\log(X/H)}$$

# of atoms

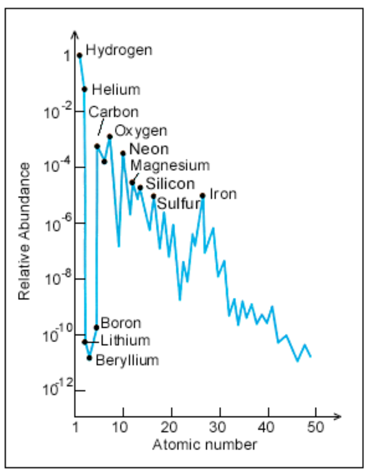

Solar Abundance from Anders & Grevesse 1989

Why 12? In 1929 Henry Norris Russell arbitrarily chose $\log(N(H))=12$

Abundance: Stars

Metal abundances in stars are defined relative to solar:

$$[\mathrm{Fe/H}] = \log_{10}\left(\frac{N_{\mathrm{Fe}}}{N_{\mathrm{H}}}\right)_{star} - \log_{10}\left(\frac{N_{\mathrm{Fe}}}{N_{\mathrm{H}}}\right)_{sun}$$

# of atoms

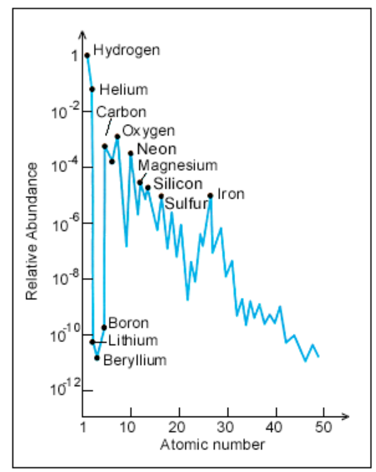

Can use any other species for "Fe" or "H" (i.e. [O/H], [O/Fe], etc)

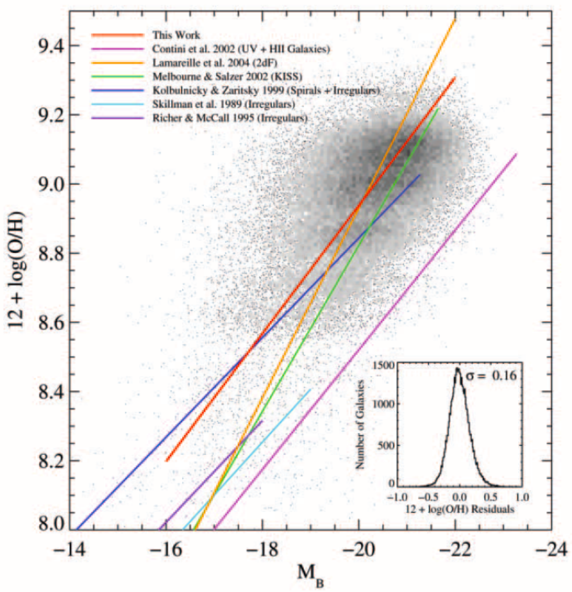

Galaxies follow a luminosity-metallicity relation

53,400 SDSS galaxies: Note -- these metallicities are biased high

Tremonti et al 2004

Mass-Metallicity Relation: Extends to very low masses

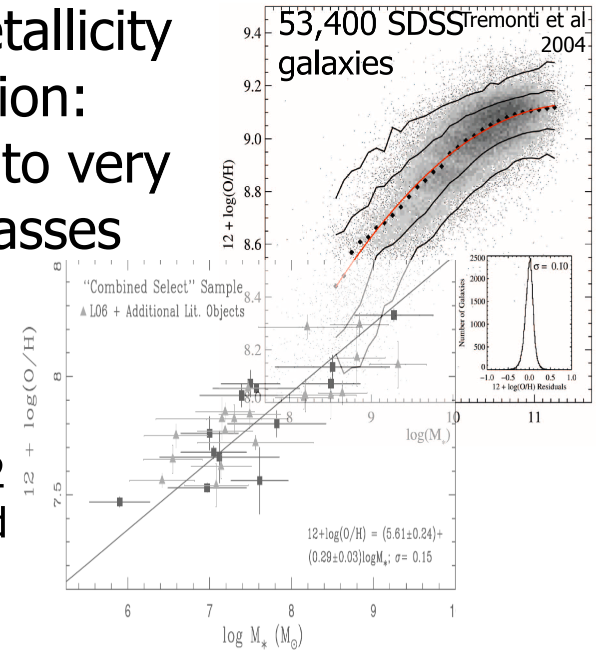

Berg et al 2012 Weak-line "gold standard" metallicities

Two Ingredients Needed:

Where do metals come from?

What "chemical evolution" sets the observed metallicity of a galaxy

Main Nucleosynthetic Channels

Stellar interior processing

Nucleosynthesis in Stars

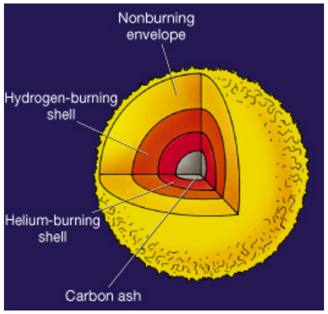

Low mass stars:
C or C+O core fuses up to Fe-peak when ignites

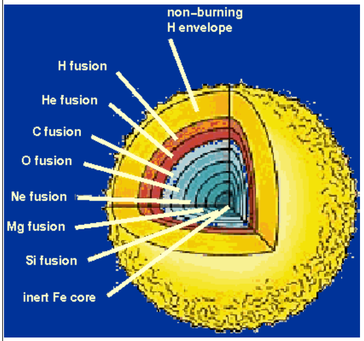

$$^{12}_{6}\mathrm{C} + ^{4}_{2}\mathrm{He} \longrightarrow ^{16}_{8}\mathrm{O} + \gamma$$
$$^{16}_{8}\mathrm{O} + ^{4}_{2}\mathrm{He} \longrightarrow ^{20}_{10}\mathrm{Ne} + \gamma$$
$$^{20}_{10}\mathrm{Ne} + ^{4}_{2}\mathrm{He} \longrightarrow ^{24}_{12}\mathrm{Mg} + \gamma$$
$$^{24}_{12}\mathrm{Mg} + ^{4}_{2}\mathrm{He} \longrightarrow ^{28}_{14}\mathrm{Si} + \gamma$$
$$^{28}_{14}\mathrm{Si} + ^{4}_{2}\mathrm{He} \longrightarrow ^{32}_{16}\mathrm{S} + \gamma$$
$$^{32}_{16}\mathrm{S} + ^{4}_{2}\mathrm{He} \longrightarrow ^{36}_{18}\mathrm{Ar} + \gamma$$
$$^{36}_{18}\mathrm{Ar} + ^{4}_{2}\mathrm{He} \longrightarrow ^{40}_{20}\mathrm{Ca} + \gamma$$
$$^{40}_{20}\mathrm{Ca} + ^{4}_{2}\mathrm{He} \longrightarrow ^{44}_{22}\mathrm{Ti} + \gamma$$
$$^{44}_{22}\mathrm{Ti} + ^{4}_{2}\mathrm{He} \longrightarrow ^{48}_{24}\mathrm{Cr} + \gamma$$
$$^{48}_{24}\mathrm{Cr} + ^{4}_{2}\mathrm{He} \longrightarrow ^{52}_{26}\mathrm{Fe} + \gamma$$
$$^{52}_{26}\mathrm{Fe} + ^{4}_{2}\mathrm{He} \longrightarrow ^{56}_{28}\mathrm{Ni} + \gamma$$

High mass stars:
α-elements through "α-ladder"

Main Nucleosynthetic Channels

Stellar interior processing

"r-process" due to rapid accretion of neutrons, followed by subsequent β-decay to stable nuclei (starts w/ Fe)

"s-process" due to slow accretion of neutrons interspersed with decay to stable nuclei (starts w/ Fe)

Cosmic ray spallation (induces fission)

r-process in action

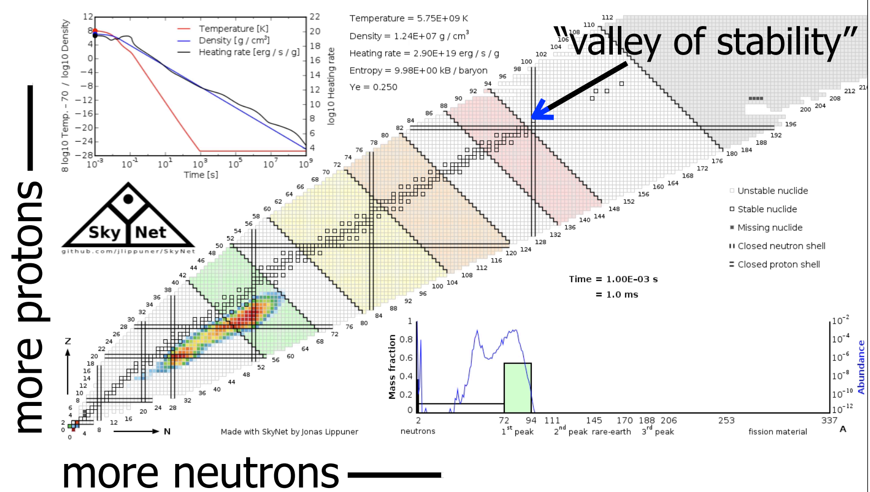

NS-NS merger kilonova simulation: https://stellarcollapse.org/lippunerroberts2015

r- and s-process produce different enrichment patterns

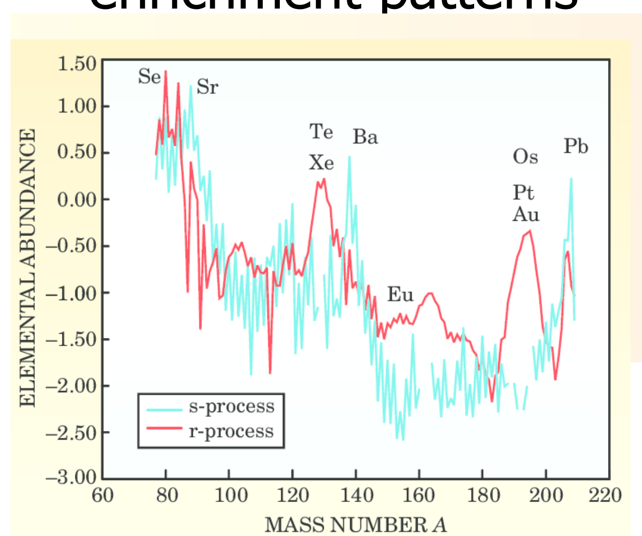

Cowan & Thielemann 2004

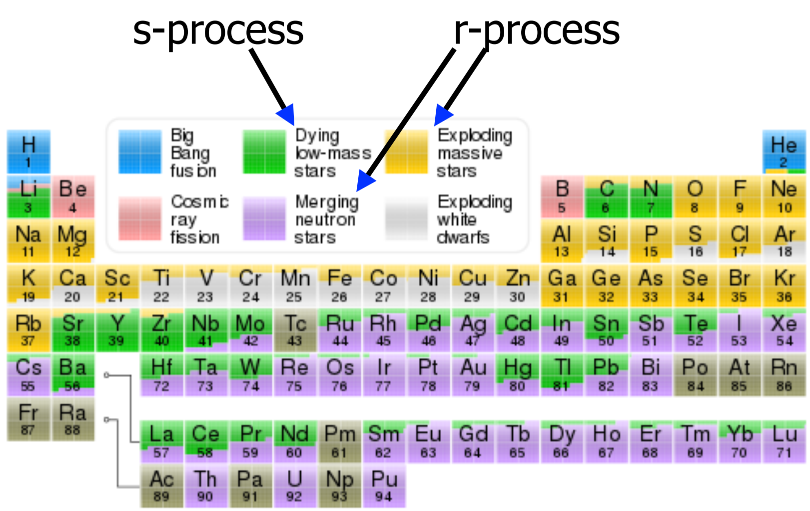

 https://en.wikipedia.org/wiki/S-process

Production of Elements I.

Type II SNe ($M > 6$-$8\ M_\odot$)

Fast enrichment (<50 Myrs)

α-element enhanced compared to solar (O, Ne, Mg, Si, S, Ar, Ca, Ti, Cr)

Type Ia SNe (Range of masses)

Some prompt, but most delayed

Fe-peak elements are dominant products

Both produce r-process elements beyond iron peak

Production of Elements II

AGB Winds (Range of masses)

Important for s-process (slow neutron capture) elements beyond Fe-peak

Pulsation + dredging

Neutron Star Mergers?

Timescale depends on binary evolution

Can also produce r-process elements

Rarer, but bigger yield per event than SNe

Produces dispersion in r-process/Fe at low Fe

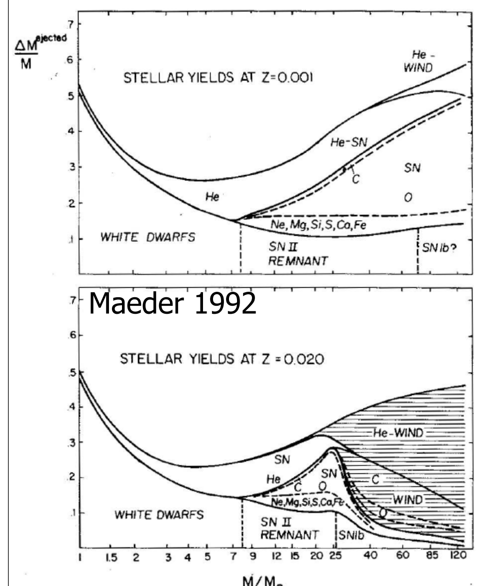

Massive Star Element Production

- Depends on Z & Mstar mass of star
- Need to integrate over IMF to get total production
- Oxygen and other α elements (Mg, Si, Ca, Ti) dominate
- Some elements from internal fusion, some in explosion

Shading: Lost in winds prior to SNe

Exact Type II yield is uncertain

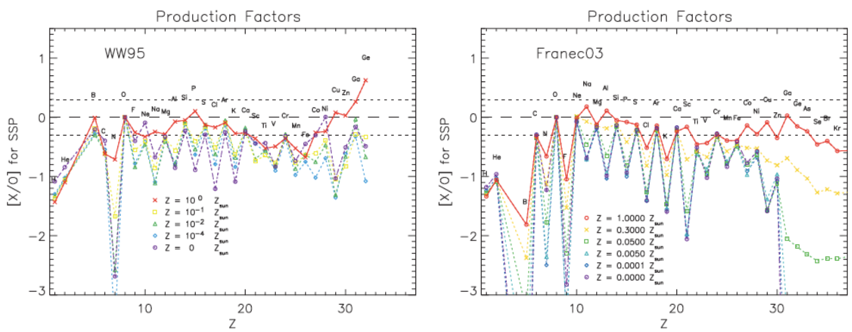

Figure 1 Production factors relative to O on a solar logarithmic scale from a single generation of massive stars using the metallicity-dependent yields of Woosley & Weaver 1995 (left panel) and those of FRANEC 2003 (right panel). The latter were kindly provided by A. Chieffi (2003, personal communication). Yields were integrated over a Salpeter (1955) IMF from 12 to 40 $M_{\odot}$. The dashed line indicates the solar values (where $\log(N_O/N_H)_{\odot} + 12 = 8.73$, Holweger 2001) and dotted lines indicate deviations from scaled solar by a factor of two. For both sets of yields C, N, and some of the iron-peak elements are subsolar because they require additional sources such as lower mass stars and Type Ia SNe. The strength of the 'odd-even' effect increases with decreasing metallicity in both cases, however the effect is more pronounced for FRANEC 2003.

Depends on nucleosynthetic models, metallicity, IMF

From review by Gibson et al 2003

Type Ia Yields: Primarily Iron Peak

Travaglio et al 2004

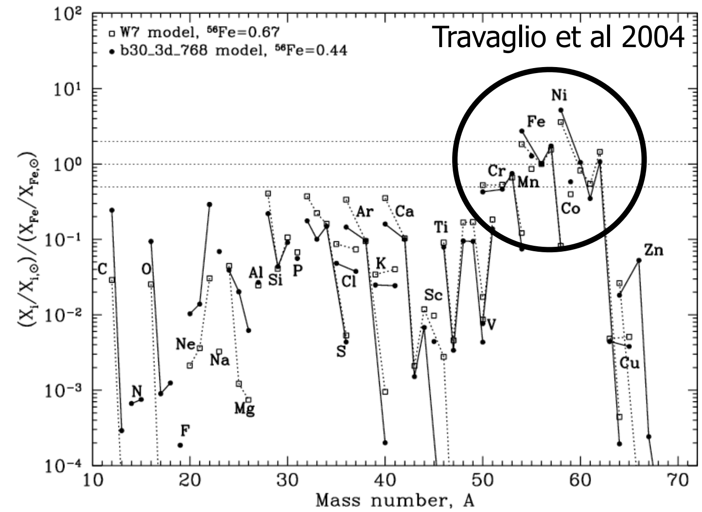

Note: Explosion models uncertain

Solar abundunce is combination of Type II, Type Ia, and s-process

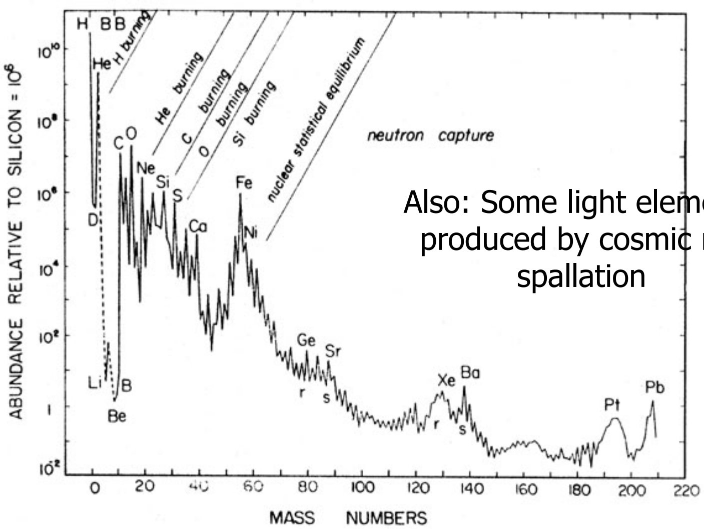

Also: Some light elements produced by cosmic ray spallation

Enrichment patterns

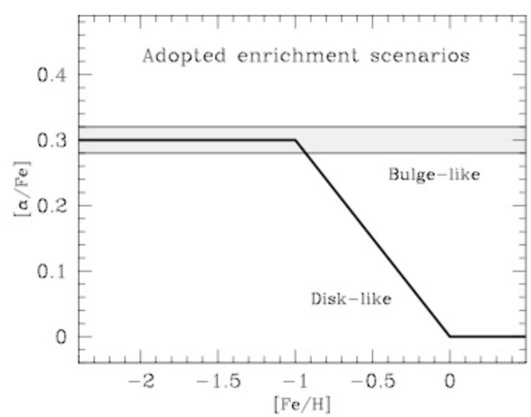

FIG. 1.—Sketched diagram of the [α/Fe] vs. [Fe/H] trend in the disk-/bulge-like enrichment scenarios, as adopted in our computational routine.

Fast enrichment: no time for Type Ia, so only Type II products

Slow enrichment: Extended SF history allows enrichment of Type II iron peak elements

Galaxy history affects patterns

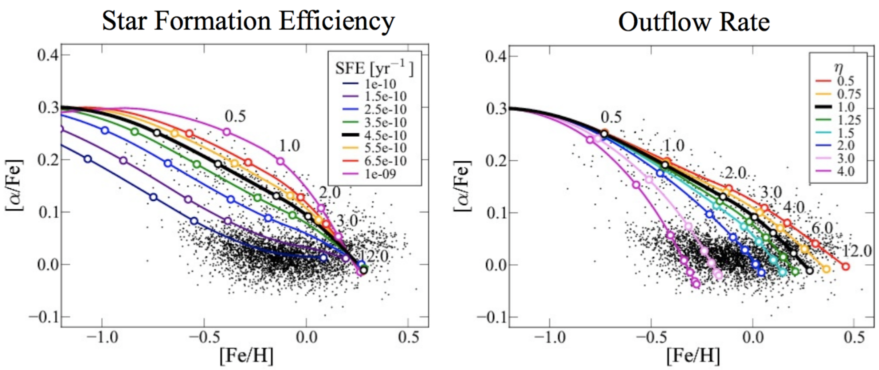

Andrews et al 2015 (in prep)

Application: Stars in Milky Way

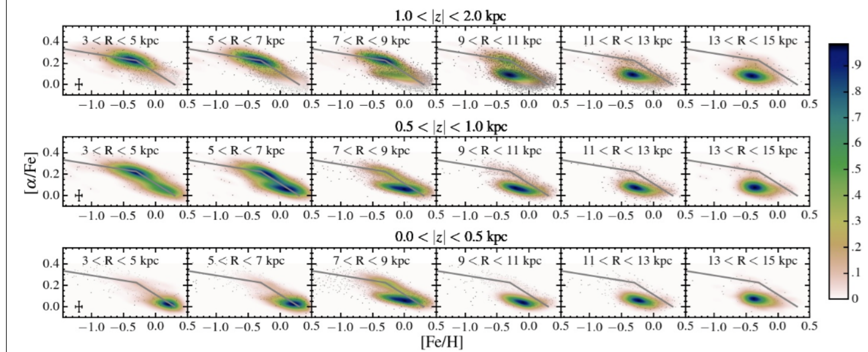

Figure 4. The stellar distribution of stars in the [α/Fe] vs. [Fe/H] plane as a function of R and $|z|$. **Top:** The observed [α/Fe] vs. [Fe/H] distribution for stars with $1.0 < |z| < 2.0$ kpc. **Middle:** The observed [α/Fe] vs. [Fe/H] distribution for stars with $0.5 < |z| < 1.0$ kpc. **Bottom:** The observed [α/Fe] vs. [Fe/H] distribution for stars with $0.0 < |z| < 0.5$ kpc. The grey line on each panel is the same, showing the similarity of the shape of the high-[α/Fe] sequence with R. The extended solar-[α/Fe] sequence observed in the solar neighborhood is not present in the inner disk ($R < 5$ kpc), where a single sequence starting at high-[α/Fe] and low metallicity and ending at solar-[α/Fe] and high metallicity fits our observations. In the outer disk ($R > 11$ kpc), there are very few high-[α/Fe] stars.

APOGEE: Higher α-enhancement above the plane, and towards the center of the galaxy. Faster SF.

Hayden et al 2015

Application: Stars in dwarfs

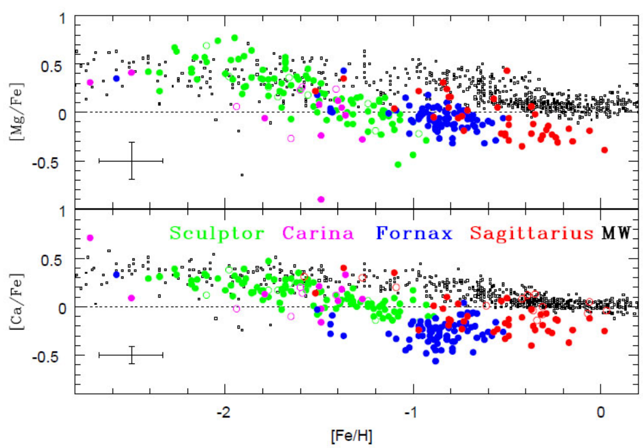

Dwarfs: Fe enrichment does not progress as far before SN II α-enhancement becomes diluted. Winds?

Venn et al 2004

What sets galaxy metallicity?

"Chemical Evolution"

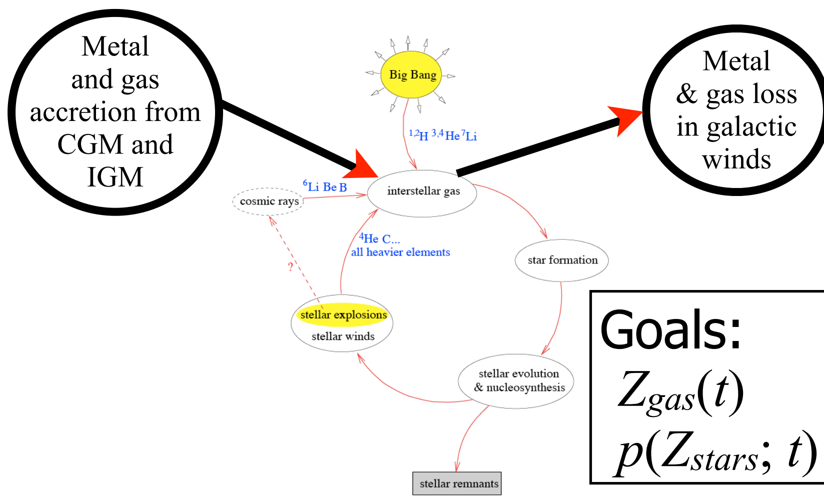

Goals:

$Z_{gas}(t)$

$p(Z_{stars}; t)$

Complex accounting problem

Masses

M_g: Total mass of interstellar gas
M_s: Total mass of stars
M_w: Total mass of stellar remnants (white dwarfs)
M_t: Total mass of the system
$M_t = M_g + M_s + M_w$

Rates

E: the rate of mass ejection from stars
E_Z: the rate of metal ejection from stars
W: the creation rate of stellar remnants.
Ψ: Rate of star formation
f: Rate of infall or outflow of material from the system
Z_f: Metal abundance of the infall (or outflow) material
$\phi(m)$: the Initial Mass Function

Stellar Evolution & Nucleosynthesis

w: the mass of a stellar remnant
τ_m: the main-sequence lifetime of a star
m_{tn}: the turnoff mass of a population with $t = \tau$
p_z: the stellar recyclable mass fraction that is converted to metal z and then ejected into space.

Classic references: Tinsley 1980 (Fundamentals of Cosmic Physics)
Pagel 1997 (Textbook)

Key, unfamiliar quantities:

Return Fraction (R)	The mass fraction of a generation of stars that is returned to the ISM. Depends on time, but typically 0.2-0.3
Lock up fraction ($\alpha = 1\text{-}R$)	The mass fraction of a generation of stars that is locked up in long-lived stars or remnants.
"Nucleosynthetic yield" (y or p)	The mass in newly formed elements ejected by a generation of stars, in units of the mass locked up in long-lived stars and stellar remnants

Simplest Form: "Closed Box"

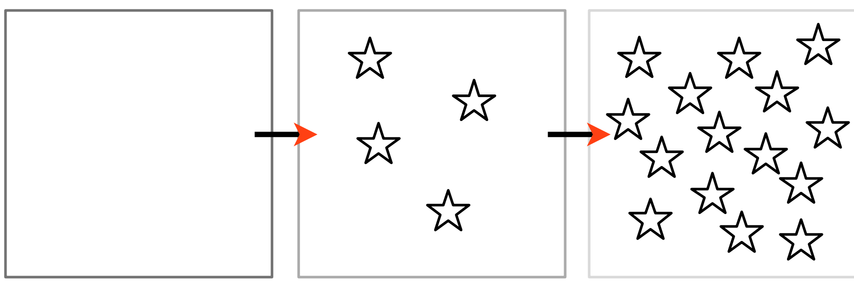

$Z_{\rm gas} = 0$, $f_{\rm gas} = 1$ | $Z_{\rm gas} > 0$, $f_{\rm gas} = 0.5$ | $Z_{\rm gas} \gg 0$, $f_{\rm gas} = 0.1$

No infall or outflow
Assume "instantaneous recycling" for massive stars

Searle & Sargent 1972

Closed Box Model

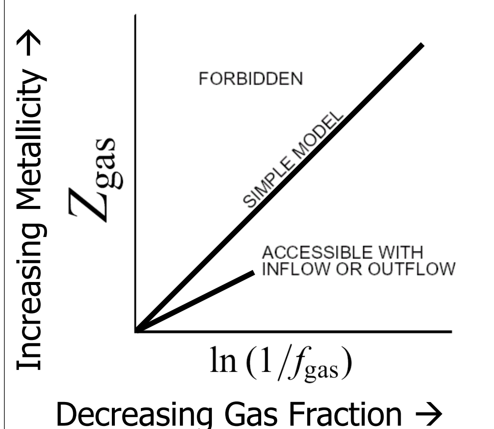

$f_{\rm gas}$ = gas fraction = $M_{\rm gas}/M_{\rm baryon}$

$$\boxed{Z = y_Z \ln(\mu^{-1})}$$

Nucleosynthetic "yield"

$$\boxed{y_{\rm eff} = \frac{Z({\rm obs})}{\ln(\mu^{-1})}}$$

"Effective Yield"

 Edmunds 1990

If $y_{eff} \sim y_Z$, evolved like "closed box"

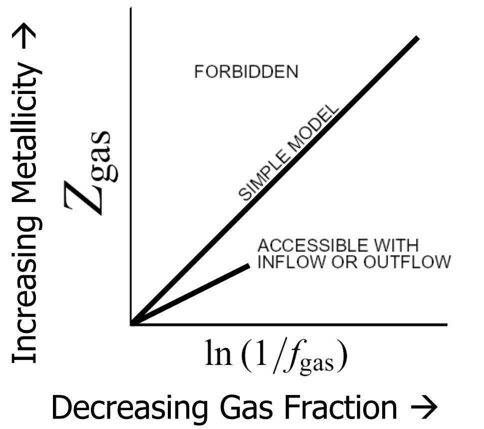

$$Z = y_Z \ln(\mu^{-1})$$

Nucleosynthetic "yield"

$$y_{eff} = \frac{Z(\text{obs})}{\ln(\mu^{-1})}$$

"Effective Yield"

f_{gas} = gas fraction = M_{gas}/M_{baryon}

 Edmunds 1990

Deviations from closed box

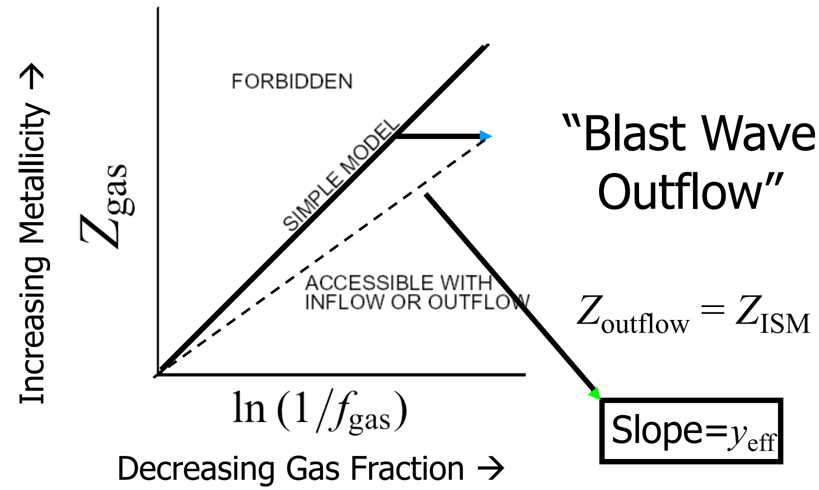

Loses "typical" gas

Deviations from closed box

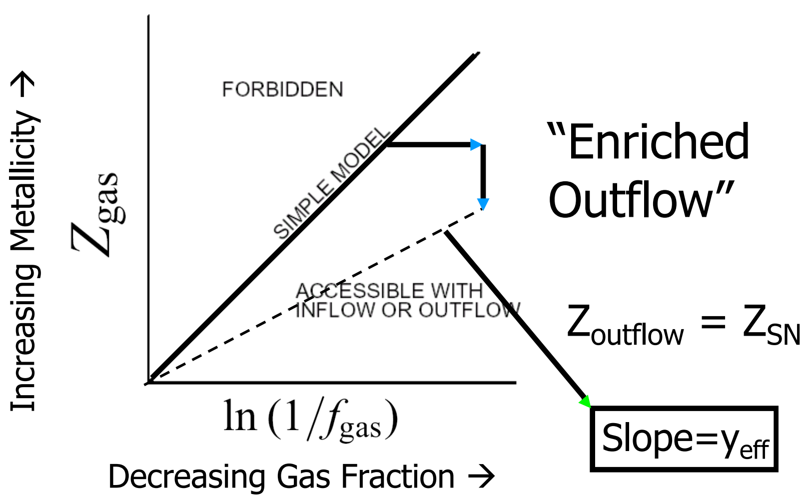

Loses metal-rich gas (SNe ejecta)

Deviations from closed box

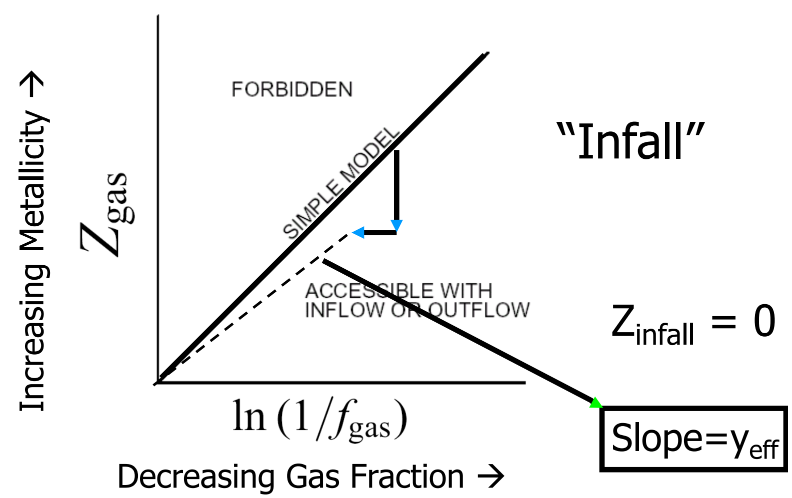

Accretes metal-poor gas (IGM)

Mass-Metallicity vs Effective Yield

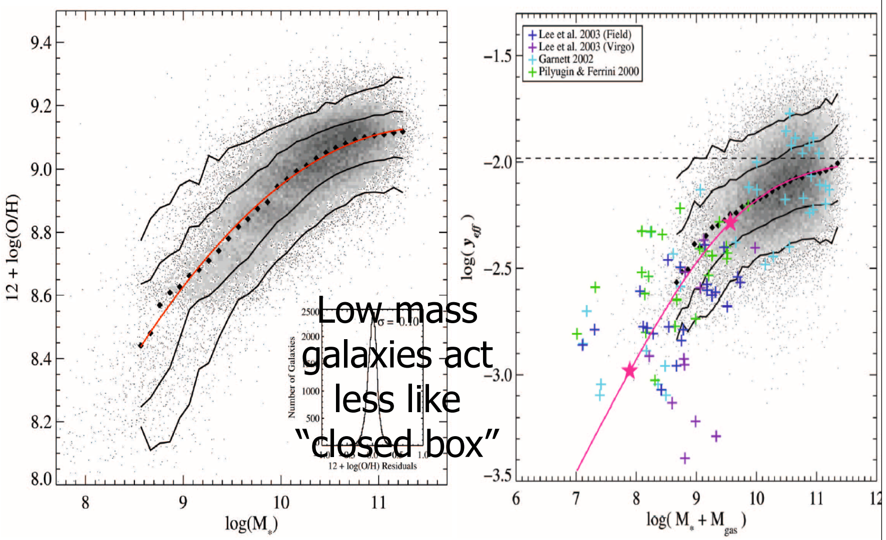

Low mass galaxies act less like "closed box"

33

Mass-Metallicity vs Effective Yield

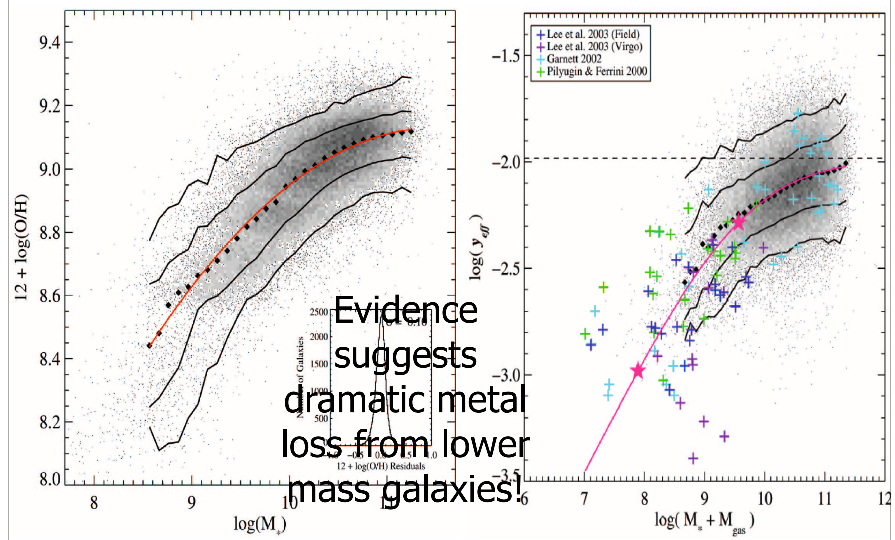

Evidence suggests dramatic metal loss from lower mass galaxies!

But note, metal loss != gas mass loss

34

Effective yield is constant for V > 120 km/s

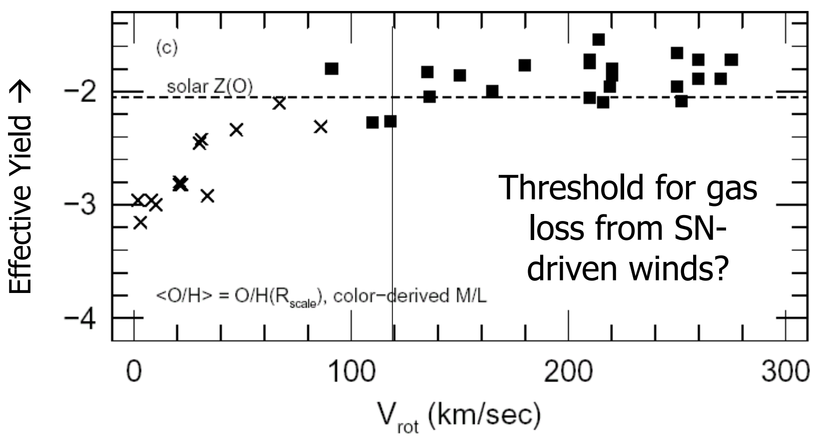

Threshold for gas loss from SN-driven winds?

Garnett 2002

35

No. It's just hard to change effective yield of gas poor systems

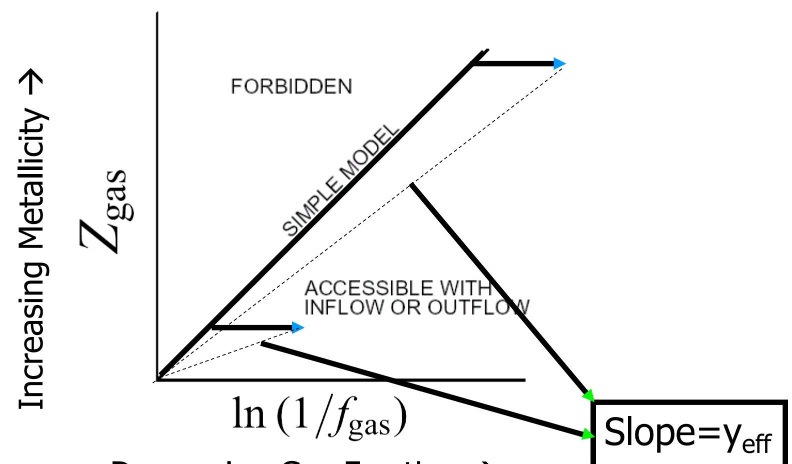

Dalcanton 2007

36

Inferred metal loss is high, increases steadily

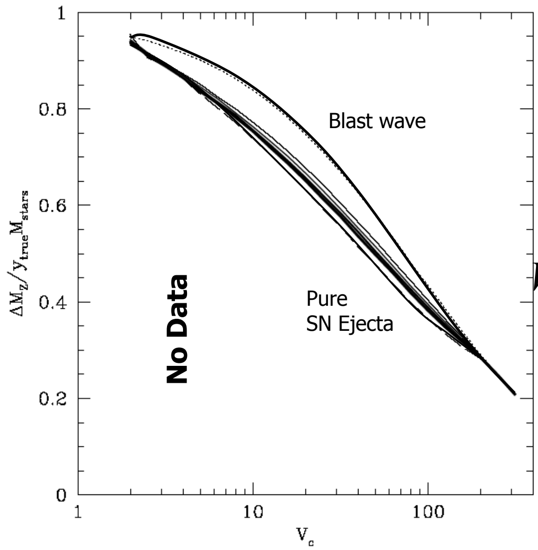

No clear feature at V_c=120km/s

For dSph and ultrafaints, more like 99% metal loss (Kirby et al 2013)

In LG dwarfs metal loss is near total

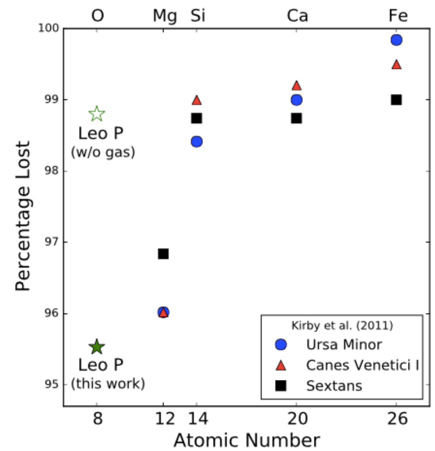

Figure 2. Percentage of O lost in Leo P compared to the percentage of metals lost in 3 Milky Way dSphs of comparable stellar mass from Kirby et al. (2011). Leo P has retained its gas content and thus a larger fraction of O. If the O atoms in the gas phase are ignored, the percentage of O lost is comparable to gas-poor dSphs (unfilled star point). Also note the discrepant low value for Mg loss in the dSphs.

- Measure stellar mass & SFH
- Infer production of elements (mass formed) M_{form}
- Measure stellar metallicities to infer mass in metals locked up M_{kept}
- Calculate M_{kept} / M_{form}

McQuinn et al 2015

Metallicity-sensitive indicators

Stars:
Tracks [Fe/H] at time luminosity-weighted stellar population formed

- Broadband colors — particularly NIR
- Spectral fitting (i.e. fit template to whole spectrum).
- Equivalent widths of specific spectral features (in absorption)

More Metals = More absorption

Ross et al 2014

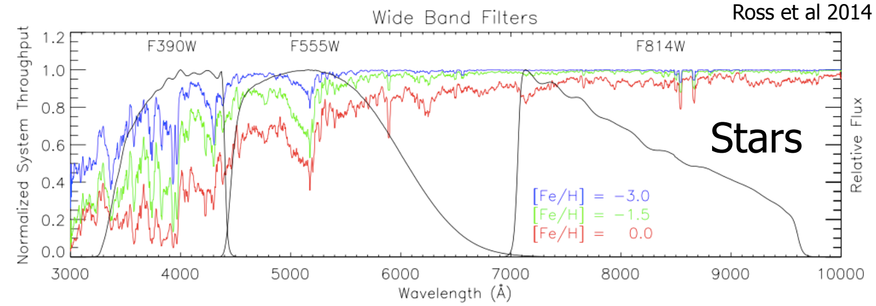

More absorption lines in the blue

Redder = More metal rich

But, age effects in composite populations

Colors more robust metallicity indicator in NIR, but spectral fitting more robust in optical

"Age-Metallicity Degeneracy"

Ross et al 2014

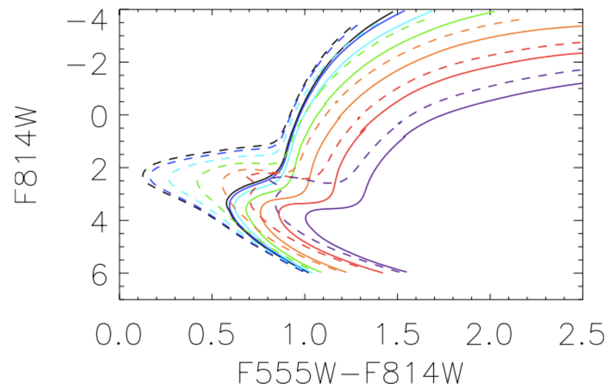

Figure 2. Age–metallicity degeneracy is shown here with isochrones of different ages covering a range of metallicity $-2.5 < [Fe/H] < +0.5$; black represents the most metal-poor, purple the most metal-rich, with each color in between representing a 0.5 increment in [Fe/H]; the solid lines represent an age of 12.5 Gyr and the dashed lines represent 4 Gyr.

Galaz et al 2002

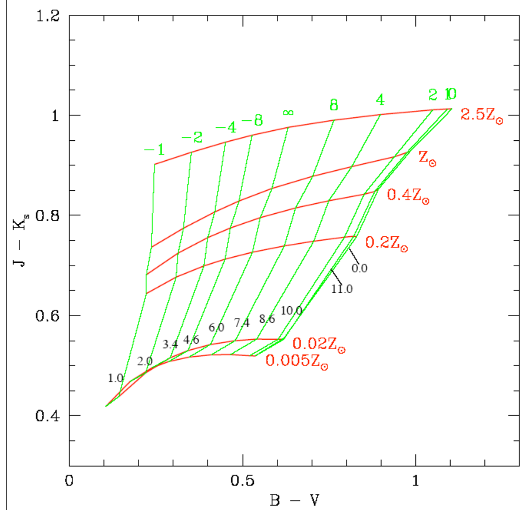

Combine colors to interpret age & metallicity

Lines of constant metallicity (red) have nearly constant J-K colors.

Lines of constant age (green) have relatively constant B-V colors

Fig. 15.— Color grid for the $J - K_s$ index as a function of the $B - V$ index, for different stellar formation rates and metallicities. Metallicities range from $0.005Z_\odot$ to $2.5Z_\odot$. Top labels denote different exponential star-formation rates, where ∞ denotes a constant star-formation rate. Bottom labels denote mean ages in Gyr. The star-formation started 12 Gyr ago for all bursts.

Caveat

Ross et al 2014

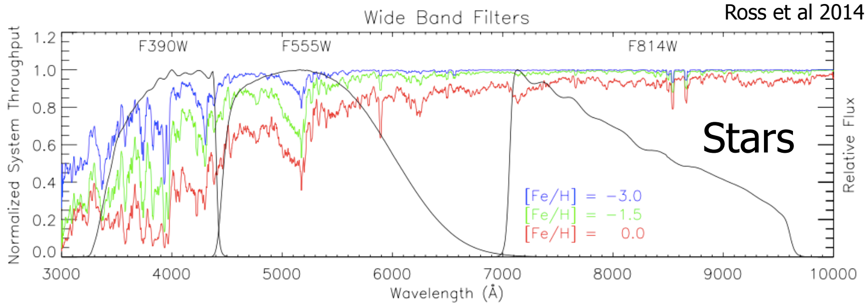

Stellar metallicity indicators are light-weighted

Different galaxies will have different age stars dominating light-weighted spectrum

Comparing stellar metallicity is not tracking identical age across galaxies.

Caveat: Color also depends on abundance patterns

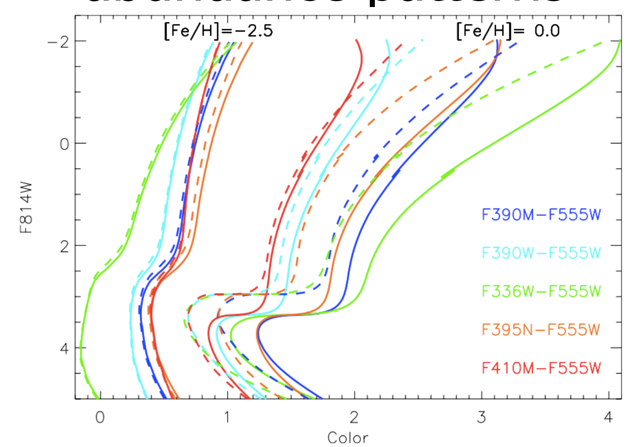

Figure 7. Color changes due to shifts in α at low and high metallicity for five metallicity-sensitive colors listed. The solid and dashed lines represent $[\alpha/Fe] = +0.4$ and 0.0 at $[Fe/H] = -2.5$, and $[\alpha/Fe] = +0.2$ and -0.2 at $[Fe/H] = 0.0$.

Ross et al 2014

INDEX DEFINITIONS

Name (2)	Index Bandpass (3)	Pseudocontinua (4)	Units (5)	Measures[a] (6)
CN_1	4142.125–4177.125	4080.125–4117.625 4244.125–4284.125	mag	C, N, (O)
CN_2	4142.125–4177.125	4083.875–4096.375 4244.125–4284.125	mag	C, N, (O)
Ca4227	4222.250–4234.750	4211.000–4219.750 4241.000–4251.000	Å	Ca, (C)
G4300	4281.375–4316.375	4266.375–4282.625 4318.875–4335.125	Å	C, (O)
Fe4383	4369.125–4420.375	4359.125–4370.375 4442.875–4455.375	Å	Fe, C, (Mg)
Ca4455	4452.125–4474.625	4445.875–4454.625 4477.125–4492.125	Å	(Fe), (C), Cr
Fe4531	4514.250–4559.250	4504.250–4514.250 4560.500–4579.250	Å	Ti, (Si)
$C_2$4668	4634.000–4720.250	4611.500–4630.250 4742.750–4756.500	Å	C, (O), (Si)
Hβ	4847.875–4876.625	4827.875–4847.875 4876.625–4891.625	Å	Hβ, (Mg)
Fe5015	4977.750–5054.000	4946.500–4977.750 5054.000–5065.250	Å	(Mg), Ti, Fe
Mg_1	5069.125–5134.125	4895.125–4957.625 5301.125–5366.125	mag	C, Mg, (O), (Fe)
Mg_2	5154.125–5196.625	4895.125–4957.625 5301.125–5366.125	mag	Mg, C, (Fe), (O)
Mg*b*	5160.125–5192.625	5142.625–5161.375 5191.375–5206.375	Å	Mg, (C), (Cr)
Fe5270	5245.650–5285.650	5233.150–5248.150 5285.650–5318.150	Å	Fe, C, (Mg)
Fe5335	5312.125–5352.125	5304.625–5315.875 5353.375–5363.375	Å	Fe, (C), (Mg), Cr
Fe5406	5387.500–5415.000	5376.250–5387.500 5415.000–5425.000	Å	Fe
Fe5709	5696.625–5720.375	5672.875–5696.625 5722.875–5736.625	Å	(C), Fe
Fe5782	5776.625–5796.625	5765.375–5775.375 5797.875–5811.625	Å	Cr
Na D	5876.875–5909.375	5860.625–5875.625 5922.125–5948.125	Å	Na, C, (Mg)
TiO_1	5936.625–5994.125	5816.625–5849.125 6038.625–6103.625	mag	C
TiO_2	6189.625–6272.125	6066.625–6141.625 6372.625–6415.125	mag	C, V, Sc

Metallicity Sensitive Absorption Features

"Lick Indices":

Characterize strength of optical absorption features

Age & Metallicity Sensitive

Note that the name sometimes has no connection to what elements are actually dominating the absorption!

Trager et al 1998

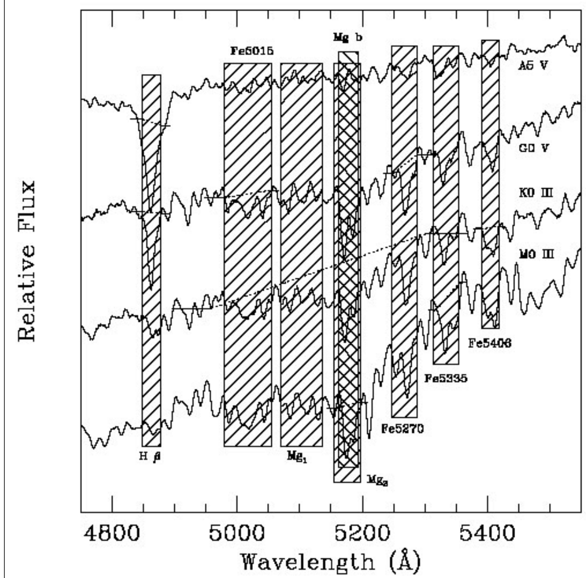

Most useful for old stellar populations

Tied to specific properties of spectrograph at Lick

Resolution & velocity-broadening dependent

Lick indices are good probes of α-enhancement for unresolved galaxies

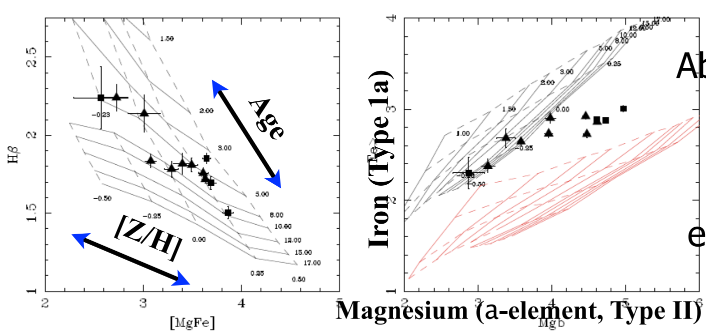

Solar Abundance

Alpha-enhanced

Figure 4. Stellar populations of Coma ETGs observed with LRIS in (Hβ, [MgFe]) and (Mg *b*, ⟨Fe⟩) space, where $[\mathrm{MgFe}] = \sqrt{\mathrm{Mg}\,b \times \langle\mathrm{Fe}\rangle}$ and $\langle\mathrm{Fe}\rangle = (\mathrm{Fe5270} + \mathrm{Fe5335})/2$. Line strengths in this figure are measured through the synthesised 2.″7-diameter aperture. Triangles are S0's, squares are ellipticals. Model grids come from the vanilla Worthey (1994) models, modified for [E/Fe] as described in the §3.1. In both panels, solid lines are isochrones (constant age) and dashed lines are isofers (constant metallicity [Z/H]). In the left panels, the models are for solar [E/Fe]; models with higher [E/Fe] have slightly lower Hβ but similar [MgFe]. Therefore this an appropriate grid from which to visually assess age and metallicity, although accurate determinations are made in (Hβ, Mg *b*, Fe5270, Fe5335) space (see text). In the right panel, grids have $[\mathrm{E/Fe}] = 0, +0.3$ (upper and lower, respectively). This is an appropriate diagram from which to visually asses [E/Fe].

Metallicity-sensitive indicators

Gas:
Tracks Z of current gas reservoir

Ratios of "strong" emission lines

Detailed fitting of weak+strong emission lines (like [OIII] "auroral" line; discussed in A541)

X-ray spectroscopy

UV absorption spectroscopy (discussed in A541)

Nice review: http://www.luth.obspm.fr/~luthier/stasinska/Stasinska.pdf

Measuring gas-phase metallicity

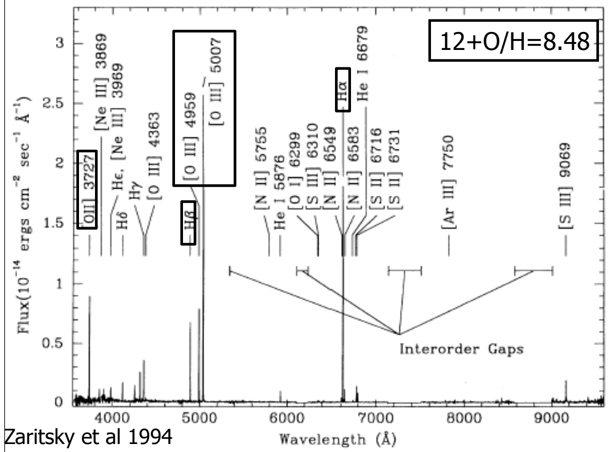

Zaritsky et al 1994

Need way of translating line ratios to elemental abundances.

Not as simple as taking ratio of O lines to H lines!

Measuring gas-phase metallicity

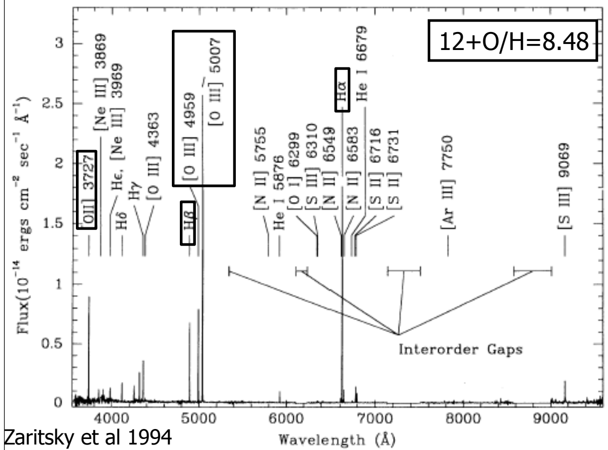

Zaritsky et al 1994

Hydrogen: recombination radiation

Oxygen: Collisionally excited forbidden lines

These are different physical processes. Their ratios don't immediately tell you much.

Measuring gas-phase metallicity

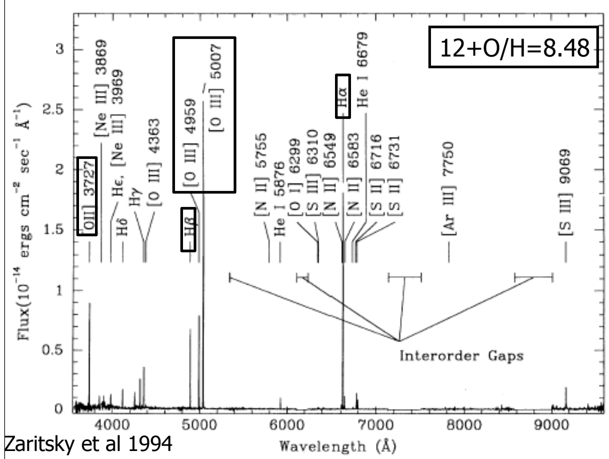

Zaritsky et al 1994

Hydrogen: recombination radiation

Line strength depends on n_e, Q_{ion} (electron density, ionizing flux).

Dependence on n_e, Q_{ion} often combined into an "ionization parameter" $U=n_\gamma/n_e$ where n_γ is # density of photons at Ly edge

Measuring gas-phase metallicity

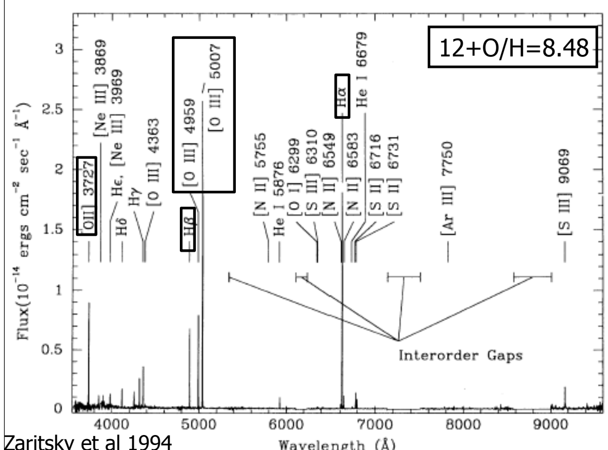

Zaritsky et al 1994

Oxygen: Collisionally* excited forbidden lines

Line strength depends on n_e, T_e (electron density, temperature)

Also will depend on degree of ionization, which also is affected by U

*Mostly. Some recombination contribution to [OII]3727Å

Example: Oxygen lines gets **stronger** in lower metallicity galaxies

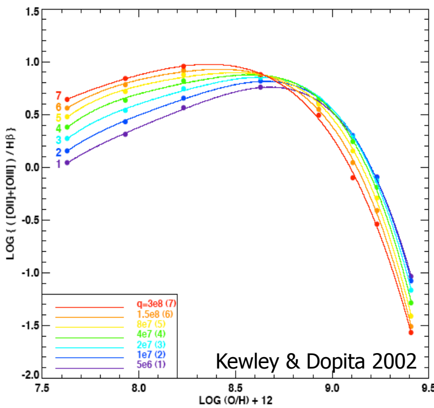

Fig. 5.— The log(([O II] λ3727 + [O III] $\lambda\lambda$4959,5007)/Hβ) (R_{23}) diagnostic for abundance versus metallicity. Curves for each ionization parameter between q = 5×10^6 to 3×10^8 cm/s are shown. Filled circles represent the data points from our models at metallicities from left to right of 0.05, 0.1, 0.2, 0.5, 1.0, 1.5, 2.0, 3.0 $Z_\odot$. This figure is available in color from the on-line version of this article.

Fewer Metals = Less Cooling
Hotter Temp = Stronger O lines

- Metal lines are the principal coolants for the ISM
- When metals are absent, cooling is inefficient
- When cooling is inefficient, the ISM is hotter
- When the ISM is hotter, upper levels of higher ionization lines are more populated

Metallicity constraints: require measuring T_e, n_e, Q_{ion}

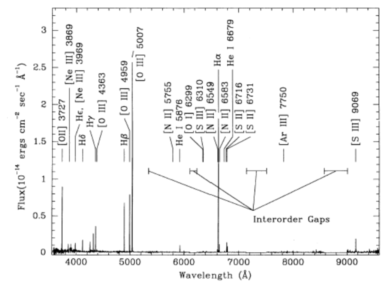

Q_{ion}: Constrain using photoionization models (usually constrains U instead)

n_e: Use "density sensitive" line ratios like [SII]6716Å,6731Å, or [OII]3727 doublet

T_e: Use "temperature sensitive" line ratios like [OIII]4363Å,5007Å

Difficulty measuring T_e with [OIII]4363Å

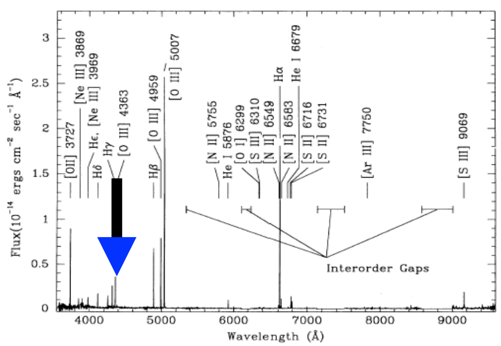

- This is a weak line! Needs high SNR
- Usual approach: Use "weak line" methods to calibrate techniques only using strong lines
- Or, use theoretical "grids" of line ratios as a function of U and Z.

"Strong Line Methods"

- "R23" method -- Uses [OII],[OIII],Hβ lines
- Pilyugin P-Method -- like R23, but with empirical correction for ionization parameter
- "N2" -- [NII]/Hα
- "O3N2" -- ([OIII]/Hβ) / ([NII]/Hα)
- "N2O2" -- [NII]/[OII]

Note: Should correct for stellar absorption lines, particular for Balmer lines

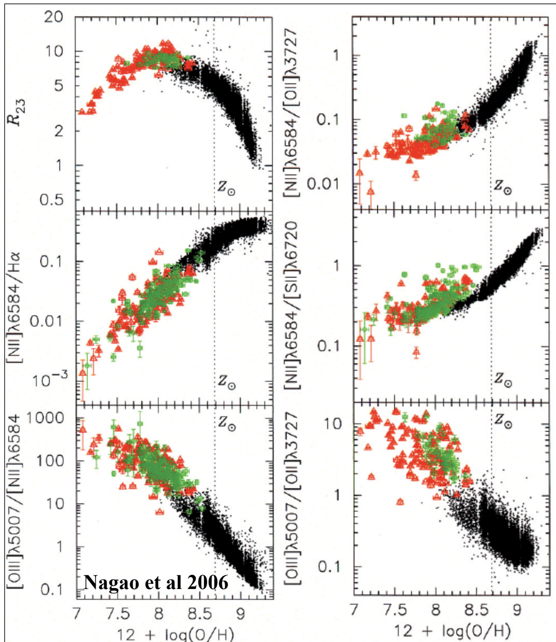

Calibrating Strong-Line Methods

Red: SDSS w/ [OIII]4363 Ivotov et al 2006

Green: Literature w/ [OIII]4363

Black: SDSS from strong lines+models

Tremonti et al 2006

Fig. 6. Emission-line flux ratios of R_{23}(=[F([OII]λ3727) + 1.327 × F([OIII]λ5007)]/F(Hβ)), F([NII]λ6584)/ F(Hα), and F([OIII]λ5007)/F([NII]λ6584) for galaxies in sample A (red triangles), in sample B (green circles) and in sample C (black dots), as a function of the oxygen abundance. The compiled low-metallicity galaxies with an error of the oxygen abundance larger than 0.05 dex are not plotted. Dotted lines denote the solar metallicity [12 + log(O/H) = 8.69].

See also Kewley & Ellison 2008

Calibrating Strong Line Methods:

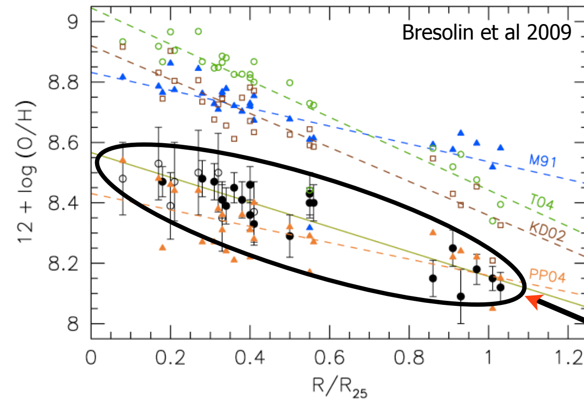

Figure 12. Galactocentric distribution of the abundance values obtained from different strong-line methods and calibrations: R_{23} (McGaugh 1991: M91, blue triangles; Tremonti et al. 2004: T04, green circles), [N II]/[O II] (Kewley & Dopita 2002: KD02, open squares), and N2 (Pettini & Pagel 2004: PP04, orange triangles). Linear least-squares fits are shown by the dashed lines, and labeled with the appropriate reference. The direct abundances determined from our work are shown by the full and open circle symbols, and the corresponding linear fit is shown by the continuous line (same as in Figure 10).

Many common strong line indicators are biased high

Ground truth from stellar spectroscopy of young stars + weak line methods

Mass-Metallicity Relation can look very different with different strong-line methods

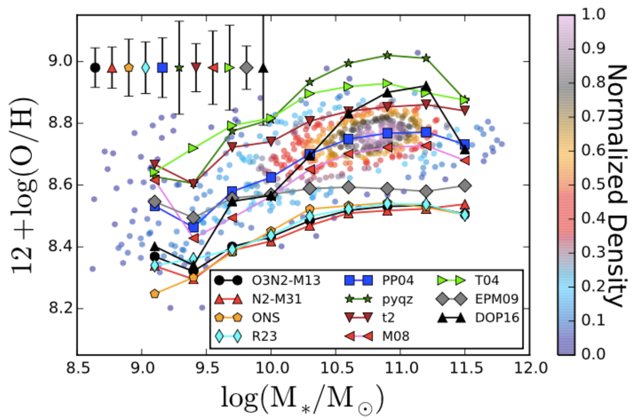

Sanchez et al 2017

Figure 3. Mass-metallicity relation derived using different oxygen abundance calibrators for the 612 galaxies extracted from the final CALIFA sample analyzed in this article, for the abundances measured at the effective radius (Reff). Colored solid symbols indicate the distribution for the individual galaxies when adopting the PP04 calibrator, with the color-code indicating the density of points (magenta indicating larger density, and light-blue indicating lower density). Line-connected symbols represent median values at a given mass bin for the different calibrators, as indicated in the inset. The error bars in the top-left symbols represent the average standard deviation for each indicator with respect to the median value at different mass bins. A description of the different calibrators is included in Sec. 3.1.

Caveats: Line ratios also affected by AGN (shocks+photoionization)

SDSS: Based on Kewley et al 2006

http://www.eso.org/~rfosbury/research/AGN2-07/AGN2-07_Messenger_v5.1.html

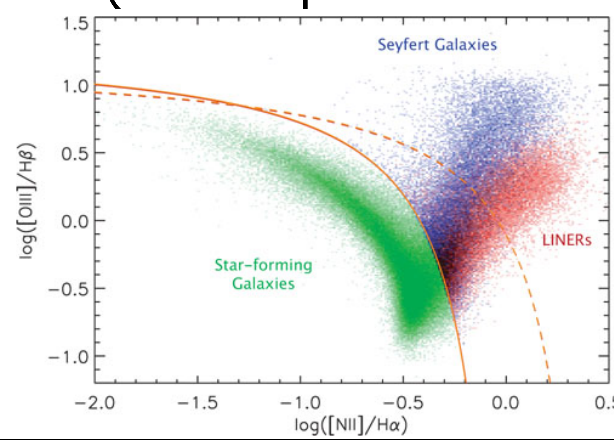

Other groups using SDSS calibration to create line ratio + color or line ratio + mass AGN vs SF galaxy classification for high-z work. (Juneau et al 2011, Yan 2011

"BPT Diagram": Baldwin, Phillips, & Terlevich 1981

Can use other lines as well. Useful for identifying AGN

Basic Metallicity Results

- Mass-metallicity correlation
  - Evidence for mass dependent metal loss
  - Possible correlation w/ SFR
  - Evolves w/ redshift
- Bulge vs disk metallicities
- Metallicity gradients within disks
- Metallicity and α-enhancement in ellipticals

Possible secondary dependence of metallicity on SFR

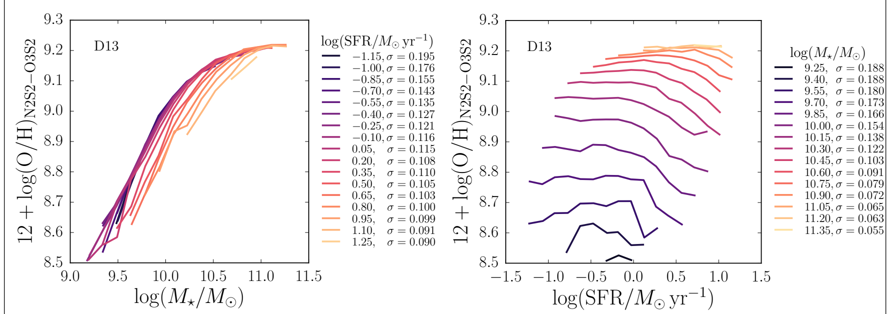

First popularized by Manucci et al 2010 (M-Z-SFR relation)

 Telford et al 2016

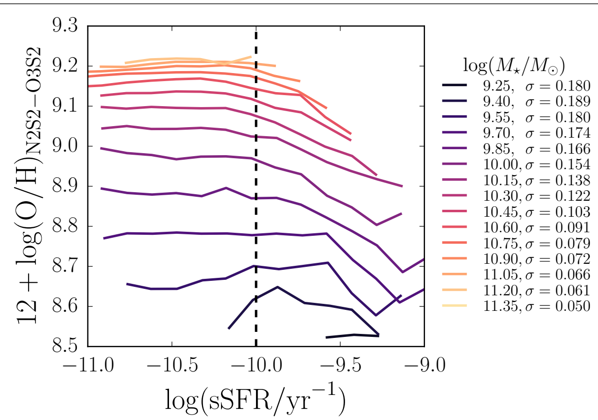

Figure 8. Recasting the $M_\star - Z -$SFR relation in terms of specific SFR. Analogous to the right panel of Figure 5 but using log(sSFR) instead of log(SFR). Metallicities are calculated using the fiducial D13 abundance diagnostic grid (N2S2–O3S2). All bins have 0.15 dex width in each $\log(M_\star)$ and log(sSFR) and each bin contains at least 50 galaxies. The dashed line at $\log(\mathrm{sSFR/yr}^{-1}) = -10$ is shown for reference; 18,960 galaxies (14.5 % of the sample) lie to the right of this line. This figure demonstrates that metallicity is only strongly anti-correlated with sSFR in the high sSFR regime.

Origin and/or strength of effect is unclear.

Some argue infall driven bursts. But, many systematics, effect weak in IFU data

 Telford et al 2016

Mass-Metallicity Evolves w/ Redshift

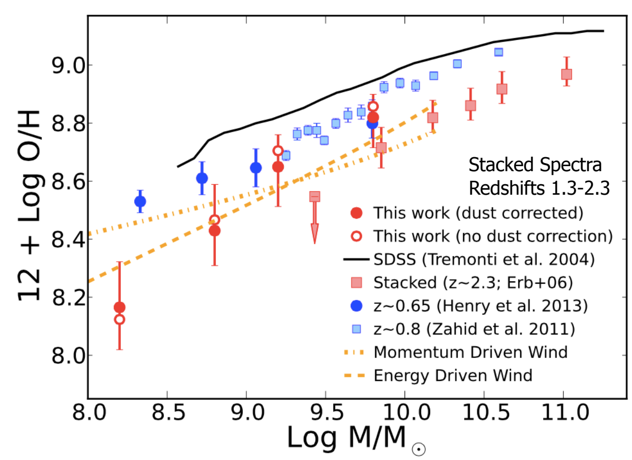

Henry et al 2013

Fraught with peril, but would be surprised if it didn't evolve.

Example: Disk vs Bulge colors

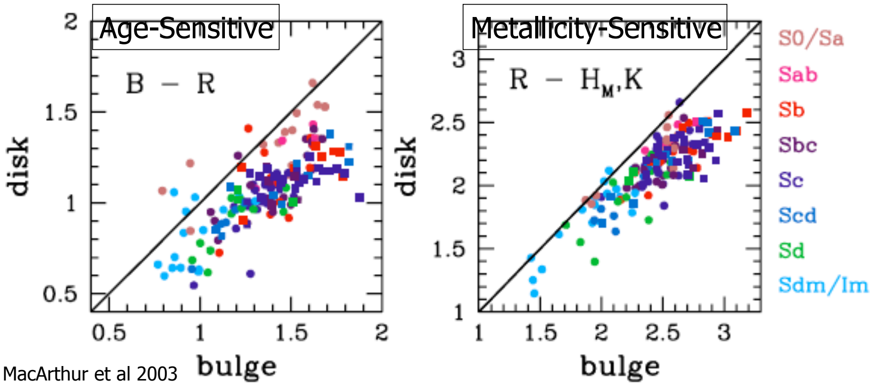

MacArthur et al 2003

Fig. 8.—Disk colors (average of 1.5–2.5 disk scale length radial bin) as a function of bulge colors (average of 0.0–0.5 disk scale length radial bin). The solid horizontal lines represent a one-to-one mapping (for reference only). H_m is the "modified" H-band magnitude for the Courteau et al. sample, converted to K band with 2MASS $H-K$ colors (see text for details) for direct comparison with the K-band data of the BdJ00 sample.

- Bulges are redder in B-R (older)
- Bulges are redder in R-K (more metal rich)

Within disks, metallicity gradients are common

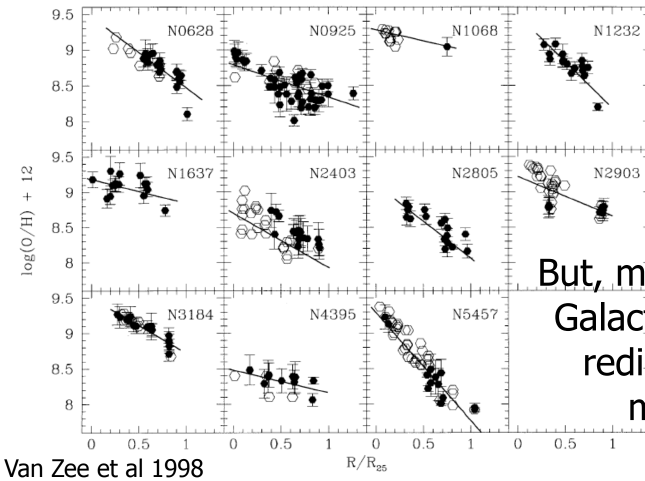

Non-zero scatter at fixed radius, however.

But, many are flat. Galactic fountain redistributing metals?

Van Zee et al 1998

Fig. 12.—Observed oxygen abundance gradients in all 11 spiral galaxies. The filled symbols represent H II regions from the present study. The open circles represent data from the literature: NGC 628, McCall et al. (1985); NGC 925, Zaritsky et al. (1994); NGC 1068, Evans & Dopita (1987), Oey & Kennicutt (1993); NGC 2403, McCall et al. (1985), Fierro et al. (1986), Garnett et al. (1997); NGC 2903, McCall et al. (1985), Zaritsky et al. (1994); NGC 3184, Zaritsky et al. (1994); NGC 4395, McCall et al. (1985); NGC 5457, Kennicutt & Garnett (1996). The solid lines illustrate the derived oxygen abundance gradients.

Internal gradients w/ stars are weaker, and dominated by age

MacArthur et al 2003

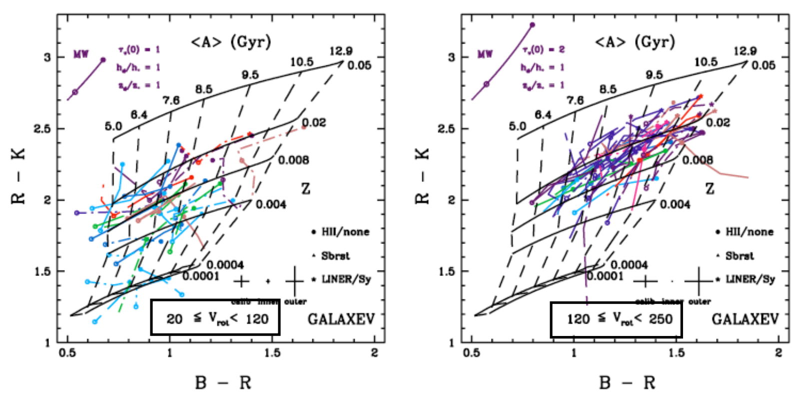

Fig. 11.—Near-IR–optical color-color plots separated by rotational velocity, V_{rot} (km s^{-1}), for the BdJ00 sample. Galaxy center point types correspond to the level of nuclear activity in the galaxies (trends with colors and their gradients with nuclear activity were looked for but none were found, possibly because of small statistics).

Is this radial differences in metal loss? in gas accretion? in gas fraction?

Application: Ellipticals in Coma

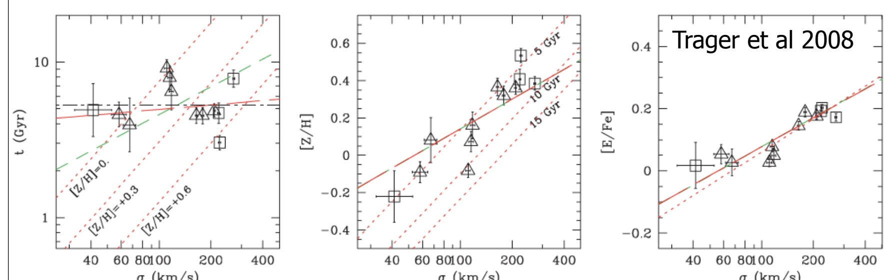

More Massive Ellipticals have:

Higher metallicity

More alpha-enhancement

(No trend with age apparent, but luminosity weighted, so small "frosting" of SF at z~0.3 could mask underlying age trend)